SAND2012-0108C

Unimolecular dissociation of hydroxypropyl and propoxy radicals

Judit Zádor[1]*, James A. Miller[2]
[1] Combustion Research Facility, Mail Stop 9055, Sandia National Laboratories, Livermore, CA 94551-0969, USA
[2] Chemistry Division, Argonne National Laboratory, Argonne, IL 60439, USA
*Corresponding author's mailing address:
Combustion Research Facility, Mail Stop 9055,
Sandia National Laboratories, Livermore, CA 94551-0969 USA
Fax: +1 (925) 294-2276
email: jzador@sandia.gov
Colloquium: Reaction kinetics
Total length of the paper determined with Method 1: 5983
Word equivalent length of main text: 3637
nomenclature: 0
references: 629
figures with caption: 1717
tables: 0
There are no figures to be reproduced in color in this manuscript.
The manuscript has accompanying electronic supplemental material.
ES1: supplfigs.pdf, contains figures S1-S3
ES2: k.dat, contains the fitted rate coefficients in CHEMKIN format
ES3: therm.dat, contains the thermo data in CHEMKIN format

Abstract
Unimolecular pressure- and temperature-dependent decomposition rate coefficients of radicals derived from *n*- and *i*-propanol by H-atom abstraction are calculated using a time-dependent master equation in the 300-2000 K temperature range. The calculations are based on a C_3H_7O potential energy surface, which was previously tested successfully for the propene + OH reaction. All rate coefficients are obtained with internal consistency with particular attention paid to shallow wells. After minor adjustments very good agreement with the few available experimental results is obtained, based on which we assess the accuracy of our calculations to be within 50%. Several interesting pathways are uncovered, such as the catalytic dehydration, well-skipping reactions and reactions forming enols. The results of the calculations can be readily used in CHEMKIN simulations or to assess important channels for higher alcohols.
Keywords: propanol, master equation, kinetics, pressure-dependence, formally direct

1. Introduction

Alcohols derived from alternative sources (biomass, algae, fungi) [1-5] are promising fuels to be used in internal combustion engines. To use these novel fuels efficiently, especially in relation to advanced engine technologies, it is necessary to predict quantitatively the early, low-temperature behavior of the chemical system [6,7], and to understand fully the major pathways leading to autoignition the fine balance among abstraction, addition, and dissociation reactions must be characterized quantitatively. Current chemical kinetic mechanisms vary significantly not only in the branching fractions for the abstraction reactions, but also in the fate of the radicals formed after abstraction. Moreover, there is practically no reliable information on the pressure- and temperature-dependence of these dissociation reactions, particularly for oxygenates.

The radicals derived from the two structural isomers of propanol provide a wide variety of relative radical-center hydroxyl-group positions; hence they can help refine our understanding of radicals derived from larger alcohols. In this work, therefore, we investigate the possible dissociation channels of all radicals derived from *n*- and *i*-propanols by H-abstraction using

RRKM-based master equation (ME) calculations. The major pathways are determined based on a detailed high-level potential energy surface, originally developed for the reaction of propene with hydroxyl radical [8]. Pressure- and temperature-dependent, channel-specific rate coefficients are also provided to be used in comprehensive chemical kinetic models, and our results readily rationalize observations such as high acetone yields in *i*-propanol flames [9].

The available information on the unimolecular decomposition reactions of hydroxypropyl and propoxy radicals is mostly experimental, it is limited to a narrow pressure and temperature range. The unimolecular dissociation of propoxy radicals has been studied experimentally mostly in the context of atmospheric chemistry (i.e. around room temperature and 1 bar), because under tropospheric conditions the alkoxy radicals are easily formed in the reaction of alkylperoxy radicals with NO. However, during the combustion of alcohols the initial radical pool is formed largely by H-abstraction reactions, and below ~900 K the alkoxy radicals are formed to a much lesser extent [10-12]. Another pathway to form alkoxy radicals during combustion is the reactions of alkyl radicals with O-atoms. Indirect information on the dissociation of C_3H_7O radicals is available from propanol flames [13-15] and jet-stirred reactor studies [16,17].

2. Construction of the potential energy surface

The starting potential energy surface (PES) used in this work for the dissociation reactions is identical to the one used for the calculations for the propene + OH system, which provided excellent agreement with all available experimental results [8,18]. The part of the PES related to *n*-propanol has four wells: α-hydroxyprop-1-yl ($CH_3CH_2C^{\bullet}HOH$, α_n), β-hydroxyprop-1-yl ($CH_3C^{\bullet}HCH_2OH$, β_n), γ-hydroxyprop-1-yl ($C^{\bullet}H_2CH_2CH_2OH$, γ_n) and *n*-propoxy ($CH_3CH_2CH_2O^{\bullet}$, O_n); on the *i*-propanol-related surface there are only three wells: α-hydroxyprop-2-yl ($CH_3CH(OH)C^{\bullet}H_2$, α_i), β-hydroxyprop-2-yl ($CH_3CH(OH)C^{\bullet}H_2$, β_i) and *i*-propoxy ($CH_3CH(O^{\bullet})CH_3$, O_i). All bimolecular exit channels are connected to the wells via a single saddle-point barrier, except the ones leading to propene + OH, which feature a saddle-point followed by a weakly bound propene…OH complex and a barrierless exit with an asymptote 2.5 kcal mol^{-1} above the saddle point. In the current work the surfaces belonging to the two isomers were treated together, because they are connected *via* the propene…OH complex.

Details of the quantum chemical calculations can be found in Ref. [8]; for easy orientation the PES is also provided in the supplementary material of the present work (Fig. S1 and S2). In short, all geometries and frequencies were optimized at the B3LYP/6-311++G(d,p) level of theory, except the tight transition states separating the *β*-hydroxypropyl wells from propene + OH, for which the B3LYP functional did not yield the correct transition states at these points. Instead, these geometries were optimized at the CAS(3e,3o)PT2/aug-cc-PVDZ level of theory. Accurate energies were obtained using the QCISD(T) quantum chemical methods with the cc-pV*n*Z basis sets, *n* = (T,Q), extrapolated to the infinite basis set limit cc-pV∞Z [19,20]. The DFT calculations were carried out with the Gaussian program package [21], while all other calculations used the Molpro suite of programs [22].

3. Calculation of rate coefficients

Pressure- and temperature-dependent rate coefficients for the dissociation and isomerization reactions on the C_3H_7O PES were calculated with the time-dependent, RRKM-based energy-resolved master equation (ME) using the Variflex code version 2.03 [23]. The ME can conveniently be written in the following form:

$$\frac{d\left|\mathbf{w}(t)\right\rangle}{dt} = \mathbf{G}\left|\mathbf{w}(t)\right\rangle \qquad (1)$$

where matrix **G** describes the chemical exchange between different wells and also the energy transfer during collisions, while vector $\left|\mathbf{w}(t)\right\rangle$ contains the unknown populations as a function of time *t*. Fourier fits to the 1-D relaxed scans at the B3LYP/6-311++G(d,p) level were used in the framework of a Pitzer-Gwinn-like approximation at the microcanonical level to take into account the hindered-rotor number and density of states [24,25] accurately. Tunneling corrections were taken into account by asymmetric Eckart transmission probabilities. Collisional energy transfer was modeled by an exponential-down model, with a temperature-dependent average downward transfer parameter $\langle\Delta E\rangle_{down}$ in the form $200 \times (T/300\ K)^{0.85}$ cm^{-1}; this parameterization gave good agreement in the fall-off region for the propene + OH addition reaction [8]. For the barrierless channels the *E*,*J*-resolved number of states were calculated variationally using the direct variable-reaction-coordinate transition-state theory [26,27] using CASPT2(5e,4o)/aug-cc-pVDZ energies. The effective flux through the barrierless entrance channel, the van der Waals well and the submerged barriers was represented by a two-transition-state model at the microcanonical, *J*-resolved level as described in detail in our previous papers [8,28].

The C_3H_7O PES features several relatively shallow wells. As a consequence, at temperatures and pressures relevant to combustion some of the well–well or some well–bimolecular product pairs might equilibrate on the time-scales of collisional energy transfer. Mathematically this phenomenon is rigorously reflected in the eigenvalue spectrum of Eq. 1. At low-enough temperatures the eigenvalues can be divided into a slow and a fast group. The slow ones, called chemically significant eigenvalues (CSE) are related to chemical reactions, while the fast ones, called internal energy relaxation eigenvalues (IERE) are related to the energy transfer processes. At elevated temperatures the gap between the two groups of eigenvalues typically decreases, and at even higher temperatures some CSE's merge into the IERE continuum, i.e. some chemical reactions take place on the same time-scale as vibrational-rotational relaxation. Pressure has a somewhat similar effect but opposite in sign. At higher pressures collisional stabilization is fast, and in the infinite-pressure-limit the thermal population is always established before any reaction takes place. At low pressures collisional relaxation is slower and the CSE's merge with the IERE's at lower temperatures.

Eq. 1 describes the dynamics on the underlying PES and the solution can be used to calculate phenomenological rate coefficients. While at sufficiently low temperatures, such as the ones encountered in atmospheric chemistry, rate coefficients can be satisfactorily established by fitting exponential decays to species time-profiles (similar to an experiment). At higher temperatures it is necessary to use more sophisticated techniques to avoid inconsistencies in the results. The two methods outlined by Miller and Klippenstein [29] are the initial-rate method and the long-time method. The initial-rate method is applicable as long as the IERE eigenvalues are much greater in magnitude than the CSE ones, or in other words, the equilibrium population in the wells is established (except perhaps for states that lie in the high-energy tail of the equilibrium distribution) before any chemical reaction would significantly perturb these populations. This can limit the use of this method to lower temperatures. The long-time method has a less stringent criterion: it is applicable as long as the magnitude of all IERE's are larger (faster) than the CSE's.

If any one of the chemically significant eigenvalues merges into the IERE quasi-continuum, both methods fail and give erroneous rate coefficients. The physical meaning of such merging is that some species (whose identity can be determined from the corresponding eigenvector) equilibrate with each other on time-scales comparable to that of the internal energy relaxation. The solution to the problem is the reformulation of the rate coefficient problem by uniting the equilibrating species into a "superspecies"; this results in new (and fewer) CSE's, which are now

separated from the IERE, at least up to higher temperatures, when a new species merging might be necessary.

Note that from a chemical modeling point-of-view these superspecies do not mean that some of the merged species are no longer present in the system. They are present at concentrations in equilibrium with each other at all times, and accordingly, their relative concentrations can be calculated through the equilibrium constant (i.e. algebraic expression) rather than solving an extra differential equation. Note also that, although the notion of superspecies can be unfamiliar, a similar idea hides behind the common practice of *not* treating conformers as separate species in a chemical mechanism, because usually IVR is much faster than processes involving the breaking and making of bonds.

5. Results

Fig. 1 shows the eigenvalue spectrum of the chemical reactions on our C_3H_7O potential energy surface as a function of temperature at 760 Torr of He. At room temperature all but one of the chemically significant eigenvalues are very small, which means that all but one chemical process is very slow. The only active eigenvalue is the one related to the propene + OH ↔ *β*-hydroxypropyl transformation; this reaction is barrierless, therefore, takes place at a substantial rate even at low temperatures, while all other reactions on this surface have a barrier, and are slow at room temperature.

Just above 300 K the dissociation of the alkoxy radicals becomes significantly faster as a result of the low barrier heights (14.3 kcal mol^{-1} for both wells). This is also reflected in the increased absolute values of the corresponding eigenvalues, and as these dissociation reactions are steeply temperature dependent, above ~850 K the two related eigenvalues merge into the IERE continuum. The trend is similar for the other eigenvalues related to dissociation, and even though the higher barriers corresponding to those reactions prevent the merging of the eigenvalues even at 2000 K, above ~1500 K the separation between most CSE's and IERE is smaller than an order of magnitude.

The remainder of the eigenvalues do not correspond to a well ↔ product process and are interesting to look at, especially that some of them change character as a function of temperature. First, there is an eigenvalue at low temperatures, which belongs to the $CH_3C^{\bullet}HCH_2OH$ ↔ $CH_3CH(OH)C^{\bullet}H_2$ process, which is not a direct reaction path on the underlying PES: these two species are not separated by a single transition state, but are connected through the two saddle points leading to the propene + OH weakly bound complex. At ~500 K this eigenvalue mixes with the propene + OH ↔ $CH_3C^{\bullet}HCH_2OH$ + $CH_3CH(OH)C^{\bullet}H_2$ one, and forms the propene + OH ↔ $CH_3C^{\bullet}HCH_2OH$ and propene + OH ↔ $CH_3CH(OH)C^{\bullet}H_2$ ones. Around this temperature all other eigenvalues become large as well, except for the propene + OH ↔ P one, which is also an eigenmode connecting species not separated by a single transition state. This eigenvalue has a close relation to well-skipping, or formally direct pathways [7,30].

Fig. 2 shows the calculated rate coefficients starting in well $CH_3C^{\bullet}(OH)CH_3$ leading to acetone + H as a function of temperature using three methods to extract rate coefficients from the ME. Below ~850 K the initial- and long-time methods give the same results, but above this temperature as the eigenvalues merge into the IERE continuum (see Fig. 1) the initial-rate method and the long-time method fail without reduction, even though the $CH_3C^{\bullet}(OH)CH_3$ well is not the one that is related to the merging. Note that between ~850 and ~900 K the long-time method continues to give positive values for the rate coefficients, and without the inspection of the eigenvalue spectrum it would be not possible to detect that these values are incorrect.

The only experimental work on the pressure-dependence of any of the reactions studied in this paper are those of Devolder et al. [31], in which the fall-off kinetics of the *i*-propoxy radical

decomposition in He in the 330-408 K temperature and 0.01-60 bar pressure range was measured. Devolder et al. fitted the experimental fall-off curves using the expression developed by Troe and coworkers [32], which gave a very good representation of the experimental data points. Fig. 3 shows the experimental data [31] and our calculated total rate coefficients as a function of pressure at the experimental temperatures. The calculated and measured values agree reasonably well, but there are two systematic discrepancies. First, the high-pressure limit rate coefficients are overpredicted by 30-50%, and the falloff appears to be slower than observed experimentally. By increasing the barrier height by 0.3 kcal mol^{-1} and by changing the $<\Delta E>_{down}$ at 300 K from 200 cm^{-1} to 150 cm^{-1}, an almost perfect agreement between theory and model is obtained. Based on this result we also increased the barrier-height for the *n*-propoxy dissociation in the full calculations by the same amount, and used $<\Delta E>_{down}$ = 150 cm^{-1} $(T/300\ K)^{0.85}$ for that well also. Such a change do not affects our previously calculated pressure-dependent rate coefficients for propene + OH [8].

Another possible reason for underpredicting the pressure-dependence is the neglect of the angular momentum conservation in the ME. Miller and Klippenstein have shown [29] that for a single-well, irreversible dissociation it is possible to solve the 2-D ME and thus test the effect of angular momentum conservation on the solution. After confirming that under the experimental conditions of Devolder et al. [31] the only accessible channel is the *i*-propoxy → acetaldehyde + CH_3 reaction, we were able to reduce the seven-well problem to a single well one. We found that the differences in the fall-off for the 1-D and 2-D calculations are very small, the 2-D calculation falling only slightly steeper (see Fig. 3).

In the following paragraphs the product channels from the individual wells are discussed. In Fig. 4 the unimolecular dissociation rate coefficients for the radicals derived from *n*-propanol, while in Fig. 5 those derived from *i*-propanol are presented at 4 Torr, 1 bar and at infinite pressure. The fitted pressure-dependent rate coefficients in the 300-2000 K temperature range on the 4 Torr, 0.1 bar, 1 bar, 10 bar, 100 bar and infinity pressure-grid are given in the supplementary material in CHEMKIN format [33]. The fitting error is always <20% (typically <5%), when the rate coefficients have an appreciable value (>10 s^{-1}). A file containing the thermodynamic information for the wells, also in CHEMKIN format, supplements the kinetic data.

The α-hydroxypropyl radical ($CH_3CH_2C^{\bullet}HOH$) derived from *n*-propanol (Fig. 4a) forms mostly vinyl alcohol + CH_3 in a β-scission step. The barrier height for this step is 31.0 kcal mol^{-1}, and the next lowest barriers belong to the formation of propanal + H (34.5 kcal mol^{-1}) and 1-propenol + H (34.6 kcal mol^{-1}). Interestingly, the most favored product channel for the α-hydroxy radical derived from *i*-propanol ($CH_3CH(OH)C^{\bullet}H_2$) is not a β-scission at a C-H bond (this would give 2-propenol + H and has a barrier of 36.8 kcal mol^{-1}), but rather at the O-H one forming acetone + H with a barrier of 32.2 kcal mol^{-1} (Fig. 5a). The striking difference between the two α-hydroxy radicals shows how dramatically a slight change in the structure can affect the favored reaction channel. There is no direct experimental information about the decomposition of the α-hydroxypropyl radicals in the literature.

Both β-hydroxy radicals form primarily propene + OH (Figs. 4b and 5b); the well depth of the β_n ($CH_3C^{\bullet}HCH_2OH$) and β_i ($CH_3CH(OH)C^{\bullet}H_2$) radicals relative to propene + OH are 27.2 and 28.2 kcal mol^{-1}, respectively. Dunlop and Tully [10] measured the rate coefficient in the *i*-propanol + OH reaction under pseudo-first-order conditions. They observed that the OH time-profiles deviate significantly from single exponential between 500 and 600 K, signaling significant OH-regeneration in the course of the abstraction reaction at elevated temperatures. They termed the following reaction sequence "catalytic dehydration":

$$CH_3CH(OH)CH_3 + OH \rightarrow CH_3CH(OH)C^{\bullet}H_2 + H_2O \quad (R1)$$

$$CH_3CH(OH)C^{\bullet}H_2 \rightarrow CH_3CHCH_2 + OH \quad (R2)$$

Using a small reaction mechanism they were able to derive the unimolecular dissociation rate coefficients for the β_i radical. Recently Kappler et al. [18] determined high-pressure limit unimolecular dissociation rate coefficients for this reaction by fitting an analytic expression to the biexponential OH time-profiles in the 600-750 K temperature range. The rate expressions derived from both works are shown in Figs. 4b and 5b and are in good agreement with theory. The most important minor channels for the β_n radical is propenol + H (33.4 kcal mol^{-1}) and allyl alcohol + H (36.8 kcal mol^{-1}). The minor channel in the β_i decomposition is vinyl alcohol + CH_3 (31.2 kcal mol^{-1}), which accounts for about 20% of the reaction products at 1000 K at the high-pressure limit. In both cases only a very small fraction of the reaction goes to the alkoxy radicals because the corresponding transition state is tight.

Fig. 3c shows the dissociation rate coefficients for the γ_n radical ($C^{\bullet}H_2CH_2CH_2OH$). The most important channel is the ethene + CH_2OH one (27.6 kcal mol^{-1}), followed by the ethyl + CH_2O one. The latter requires surmounting two consecutive barriers (24.8 kcal mol^{-1} and 18.3 kcal mol^{-1}) without stabilization in the intermediate *n*-propoxy well. This reaction channel is an example of a well-skipping (or formally direct) pathway, very characteristic of multiple-well systems [7,30,34], which can persist even at high pressures. In this case, these channels do not originate from chemical activation, but from isomerization reactions, where collisional stabilization in the intermediate wells is ineffective. The dissociation of the γ-hydroxyprop-1-yl radical can also lead to allyl alcohol + H to a smaller extent.

Finally, in Figs. 4d and 5c the channel-specific decomposition rate coefficients for the alkoxy radicals derived from propanols are shown. Due to the low barriers these species decompose faster than they can thermalize above ~850 K, the exact temperature also being dependent on the pressure. The major bimolecular product from *n*-propoxy is ethyl + CH_2O, while from *i*-propoxy it is acetaldehyde + CH_3, both formed in a simple β-scission step. The minor channels are the formation of propanal + H (*n*-propoxy) and acetone + H (*i*-propoxy). Curran [35] critically evaluated and recommended high-pressure-limit rate coefficients for these reactions, which we also present in Figs. 4d and 5c, with which our calculations generally agree well.

6. Conclusions

In this paper the dissociation pathways and their pressure- and temperature-dependent rate coefficients were presented for radicals derived from *n*- and *i*- propanols by H-atom abstraction. The model is based on our previous propene + OH calculations [8], which was in excellent agreement with a wide variety of experimental observables. In the present work all unimolecular dissociation rate coefficients were obtained simultaneously and with internal consistency by solving the time-dependent master equation with special attention paid to shallow wells on the underlying potential energy surface. Further comparisons with experimental data led to the revision of the energy transfer parameters and barrier heights for the alkoxy wells.

Our calculations point to several interesting aspects of the decomposition of radicals derived from alcohols. The α-hydroxyprop-1-yl radical decomposes primarily to vinyl alcohol via methyl radical loss, while the α-hydroxyprop-1-yl radical forms mostly acetone + H. Vinyl alcohol was found to be a major product formed in various dissociation channels. This molecule has been identified as an intermediate in *n*- and *i*-propanol flames using electron ionization and VUV-photoionization molecular-beam mass spectrometry [14]. The concentration of vinyl alcohol was reported to be ~10x more in *n*-propanol flames compared to *i*-propanol ones, which is in line with our dissociation rate coefficients and branching fractions. Our results also rationalize the high acetone concentrations observed in *i*-propanol flames.

The β-hydroxypropyl radicals follow almost exclusively the catalytic dehydration pathway leading to propene + OH. Based on the β-scission pattern of the γ-hydroxyprop-1-yl radical and

the previous calculations on the ethene + OH reaction [28] it is expected that for *n*-butanol the δ-hydroxybut-1-yl radical also constitutes to this dehydration pathway:

$$C^{\bullet}H_2CH_2CH_2CH_2OH \rightarrow C_2H_4 + C_2H_4OH \rightarrow 2\ C_2H_4 + OH \quad (R3)$$

Another dissociation pathway of the γ-hydroxyprop-1-yl constitutes a well-skipping (aka formally direct) pathway, which persist up to high pressures, forming ethyl + CH_2O. Other examples of minor well-skipping pathways can be found in the supplementary material, where rate coefficients for several channels are presented. Finally, the alkoxy radicals play a smaller role at the initial stages of alcohol combustion and these species dissociate very rapidly above ~850 K resulting.

Our work quantitatively described the dissociation pathways from the radicals derived from propanol, which can be used for both the improvement of propanol models as well as to make better predictions for larger alcohols.

Acknowledgements

This work is supported by the Division of Chemical Sciences, Geosciences, and Biosciences, the Office of Basic Energy Sciences, the U.S. Department of Energy under DOE Contract Numbers DE-AC02-06CH11357. Sandia is a multiprogram laboratory operated by Sandia Corporation, a Lockheed Martin Company, for the National Nuclear Security Administration.

References

[1] S.K. Singh, G.A. Strobel, B. Knighton, B. Geary, J. Sears, D. Ezra, Microb. Ecol. 61 (4) (2011) 729-739.
[2] G. Strobel, S.K. Singh, S. Riyaz-Ul-Hassan, A.M. Mitchell, B. Geary, J. Sears, Fems Microb. Lett. 320 (2) (2011) 87-94.
[3] G.A. Strobel, B. Knighton, K. Kluck, Y. Ren, T. Livinghouse, M. Griffin, D. Spakowicz, J. Sears, Microbiol.-Sgm 154 (2008) 3319-3328.
[4] J. Lu, C. Sheahan, P.C. Fu, Energy Environ. Sci. 4 (7) (2011) 2451-2466.
[5] T. Damartzis, A. Zabaniotou, Renew. Sust. Energ. Rev. 15 (1) (2011) 366-378.
[6] D.K. Manley, A. McIlroy, C.A. Taatjes, Phys. Today 61 (11) (2008) 47-52.
[7] J. Zádor, C.A. Taatjes, R.X. Fernandes, Prog. Energy Comb. Sci. 37 (4) (2011) 371-421.
[8] J. Zádor, A.W. Jasper, J.A. Miller, Phys. Chem. Chem. Phys. 11 (46) (2009) 11040-11053.
[9] E. Zervas, X. Montagne, J. Lahaye, Env. Sci. Tech. 36 (11) (2002) 2414-2421.
[10] J.R. Dunlop, F.P. Tully, J. Phys. Chem. 97 (24) (1993) 6457-6464.
[11] R. Sivaramakrishnan, M.C. Su, J.V. Michael, S.J. Klippenstein, L.B. Harding, B. Ruscic, J. Phys. Chem. A 114 (35) (2010) 9425-9439.
[12] C.-W. Zhou, J.M. Simmie, H.J. Curran, Combust. Flame 158 (4) (2010) 726-731.
[13] A. Frassoldati, A. Cuoci, T. Faravelli, U. Niemann, E. Ranzi, R. Seiser, K. Seshadri, Combust. Flame 157 (1) (2010) 2-16.
[14] T. Kasper, P. Osswald, U. Struckmeier, K. Kohse-Hoinghaus, C.A. Taatjes, J. Wang, T.A. Cool, M.E. Law, A. Morel, P.R. Westmoreland, Combust. Flame 156 (6) (2009) 1181-1201.
[15] P.S. Veloo, F.N. Egolfopoulos, Combust. Flame 158 (3) (2011) 501-510.
[16] C. Togbe, P. Dagaut, F. Halter, F. Foucher, Energy Fuels 25 (2011) 676-683.
[17] B. Galmiche, C. Togbe, P. Dagaut, F. Halter, F. Foucher, Energy Fuels 25 (5) (2011) 2013-2021.
[18] C. Kappler, J. Zádor, O. Welz, R.X. Fernandes, M. Olzmann, C.A. Taatjes, Z. Phys. Chem. (Neue Folge) (2011)
[19] J.M.L. Martin, Chem. Phys. Lett. 259 (5-6) (1996) 669-678.
[20] D. Feller, D.A. Dixon, J. Chem. Phys. 115 (8) (2001) 3484-3496.

[21] M.J. Frisch, G.W. Trucks, H.B. Schlegel, et al. Gaussian 09, Revision A.02; Gaussian, Inc.: Wallingford CT, 2009.
[22] H.-J. Werner, P.J. Knowles, F.R. Manby, et al. MOLPRO, version 2010.1, a package of *ab initio* programs, 2010.
[23] S.J. Klippenstein, A.F. Wagner, R.C. Dunbar, D.M. Wardlaw, S.H. Robertson, J.A. Miller. VARIFLEX; 2.03m ed., 2011.
[24] K.S. Pitzer, W.D. Gwinn, J. Chem. Phys. 10 (7) (1942) 428-440.
[25] J.A. Miller, S.J. Klippenstein, S.H. Robertson, J. Phys. Chem. A 104 (32) (2000) 7525-7536., see also J. Phys. Chem. A 2000, 7104, 9806. (correction).
[26] Y. Georgievskii, S.J. Klippenstein, J. Chem. Phys. 118 (12) (2003) 5442-5455.
[27] Y. Georgievskii, S.J. Klippenstein, J. Phys. Chem. A. 107 (46) (2003) 9776-9781.
[28] J.P. Senosiain, S.J. Klippenstein, J.A. Miller, J. Phys. Chem. A 110 (21) (2006) 6960-6970.
[29] J.A. Miller, S.J. Klippenstein, J. Phys. Chem. A 110 (36) (2006) 10528-10544.
[30] R.X. Fernandes, J. Zádor, L.E. Jusinski, J.A. Miller, C.A. Taatjes, Phys. Chem. Chem. Phys. 11 (9) (2009) 1320-1327.
[31] P. Devolder, C. Fittschen, A. Frenzel, H. Hippler, G. Poskrebyshev, F. Striebel, B. Viskolcz, Phys. Chem. Chem. Phys. 1 (4) (1999) 675-681.
[32] R.G. Gilbert, K. Luther, J. Troe, Ber. Bunsen-Ges. Phys. Chem. 87 (2) (1983) 169-177.
[33] R.J. Kee, R.M. Rupley, J.A. Miller, et al. CHEMKIN-PRO; Reaction Design, Inc.: San Diego, CA, 2008.
[34] J.P. Senosiain, S.J. Klippenstein, J.A. Miller, J. Phys. Chem. A 110 (17) (2006) 5772-5781.
[35] H.J. Curran, Int. J. Chem. Kinet. 38 (4) (2006) 250-275.

Figure captions

Figure 1. Chemically significant eigenvalues (λ) and the internal energy relaxation eigenvalue (IERE) continuum as a function of temperature at 760 Torr He pressure. The eigenvalues are labeled according to the eigenmodes; R = propene + OH, P = bimolecular products, α, β, γ and O signify the position of the radical center relative to the OH group, while the *n* and *i* subscripts mean 1-hydroxy and 2-hydroxy, respectively.

Figure 2. Rate coefficient for reaction $CH_3C^{\bullet}(OH)CH_3 \rightarrow$ acetone + H obtained with the initial rate method, the long-time method and with the long-time method with reduction at 760 Torr of He.

Figure 5. Falloff curves for the decomposition of the *i*-propoxy radical in He bath gas. The symbols are the experimental values of Devolder et al. [31] at 408, 387, 376, 363, 351, 339 and 330 K from top to bottom (digitized from the original publication), the dashed lines are the calculations with the original parameters of Zádor et al. [8], while the solid lines are with the barrier reduced by 0.3 kcal mol^{-1} and ΔE_{down}(300 K) = 150 cm^{-1}. The dotted lines (shown only for 330 and 408 K) correspond to the solution of the 2-D master equation.

Figure 4. Dissociation rate coefficients as a function of temperature at various pressures for the (a) $CH_3CH_2C^{\bullet}HOH$, (b) $CH_3C^{\bullet}HCH_2OH$, (c) $C^{\bullet}H_2CH_2CH_2OH$ and (d) $CH_3CH_2CH_2O^{\bullet}$ radicals. Note that in the high-pressure limit the γ-hydroxyprop-1-yl radical produces the *n*-propoxy radical and not the ethyl + CH_2O bimolecular product. The experiments of Kappler et al. [18] measured the total rate coefficients in the high-pressure limit. The product channels are labeled only at the high-pressure limit for clarity.

Figure 5. Dissociation rate coefficients as a function of temperature at various pressures for the (a) $CH_3C^{\bullet}(OH)CH_3$, (b) $CH_3CH(OH)C^{\bullet}H_2$ and (c) $CH_3CH(O^{\bullet})CH_3$ radicals. The product channels are labeled only at the high-pressure limit for clarity. The experiments of Kappler et al. [18] and those of Dunlop and Tully [10] measured the total rate coefficients in the high-pressure limit.

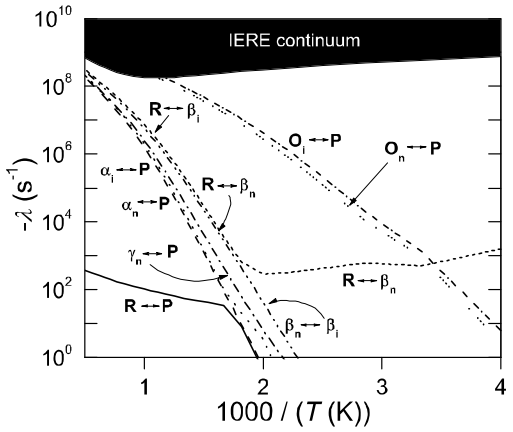

Figure 1.

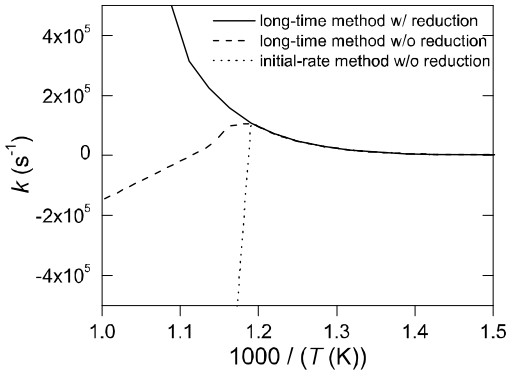

Figure 2.

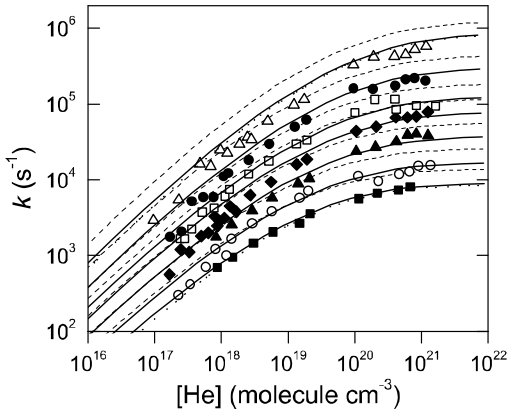

Figure 3.

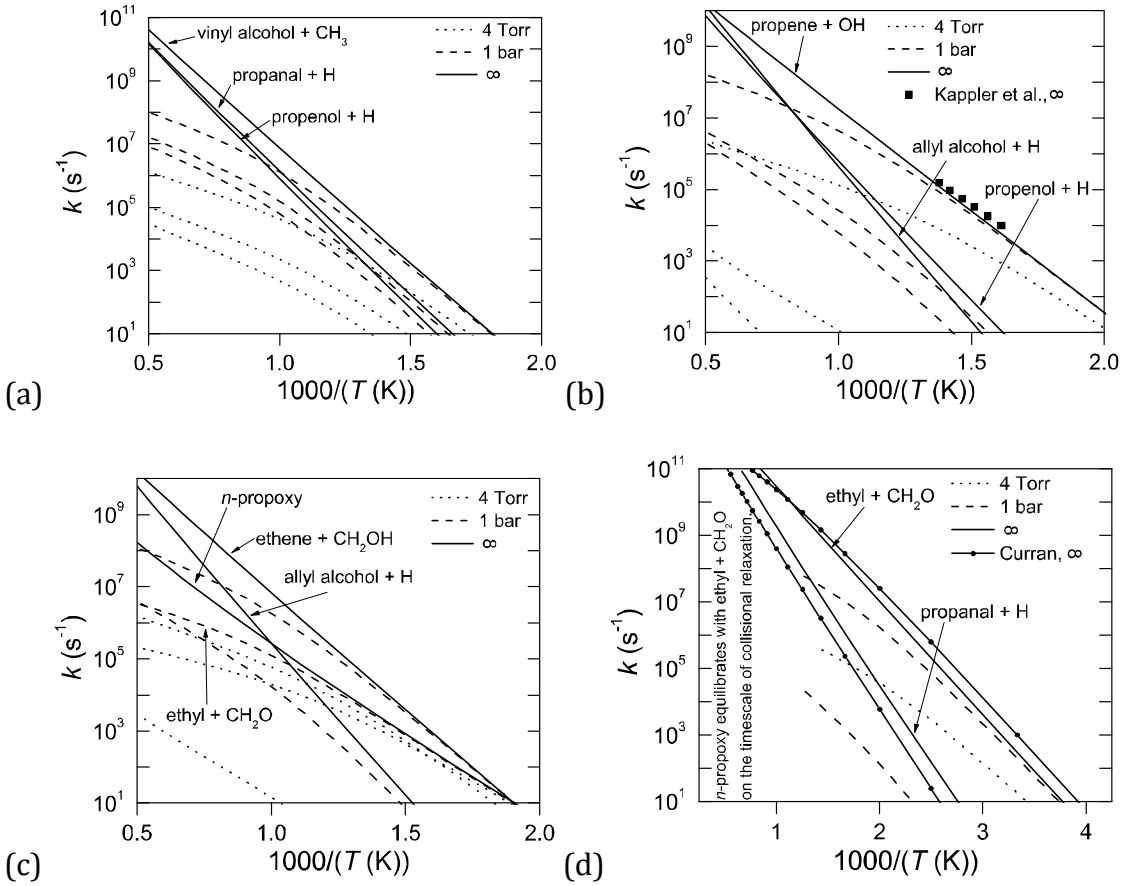
(a)
vinyl alcohol + CH3
propanal + H
propenol + H
4 Torr
1 bar
∞
k (s-1)
1000/(T (K))
(b)
propene + OH
Kappler et al., ∞
allyl alcohol + H
propenol + H
(c)
n-propoxy
ethene + CH2OH
allyl alcohol + H
ethyl + CH2O
(d)
ethyl + CH2O
Curran, ∞
propanal + H
n-propoxy equilibrates with ethyl + CH2O
on the timescale of collisional relaxation

Figure 4.

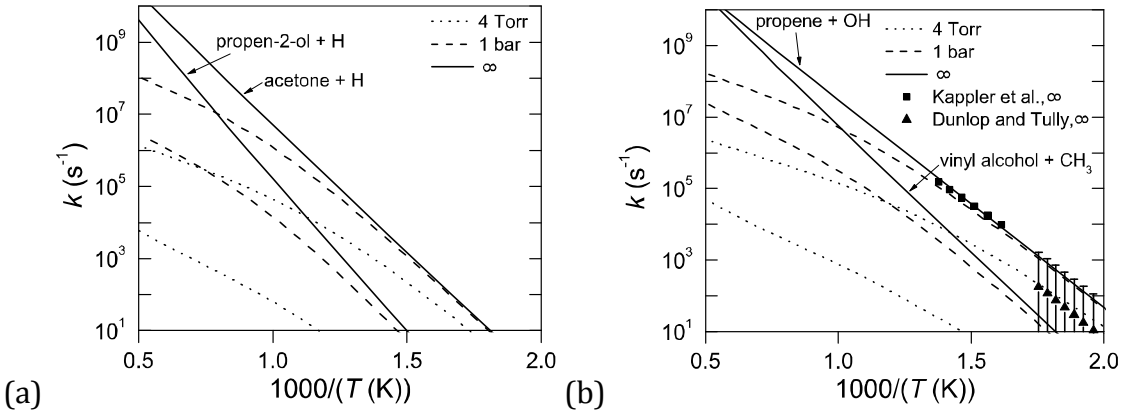
(a)
propen-2-ol + H
acetone + H
4 Torr
1 bar
∞
k (s-1)
1000/(T (K))
(b)
propene + OH
Kappler et al., ∞
Dunlop and Tully, ∞
vinyl alcohol + CH3

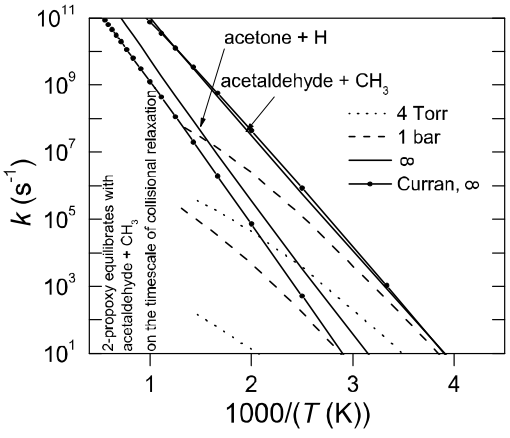
acetone + H
acetaldehyde + CH3
4 Torr
1 bar
∞
Curran, ∞
2-propoxy equilibrates with acetaldehyde + CH3 on the timescale of collisional relaxation
k (s-1)
1000/(T (K))

(c)

Figure 5.